Electronic Supplementary Material (ESI) for Physical Chemistry Chemical Physics.

Nature of aryl-tyrosine interactions contribute to β-hairpin scaffold stability: NMR evidence for alternate ring geometry

Kamlesh Madhusudan Makwana and Radhakrishnan Mahalakshmi*

Molecular Biophysics Laboratory, Department of Biological Sciences, Indian Institute of Science Education and Research, Bhopal – 462023. India.

*E-mail: *maha@iiserb.ac.in*

Supplementary Information

Supplementary Figures

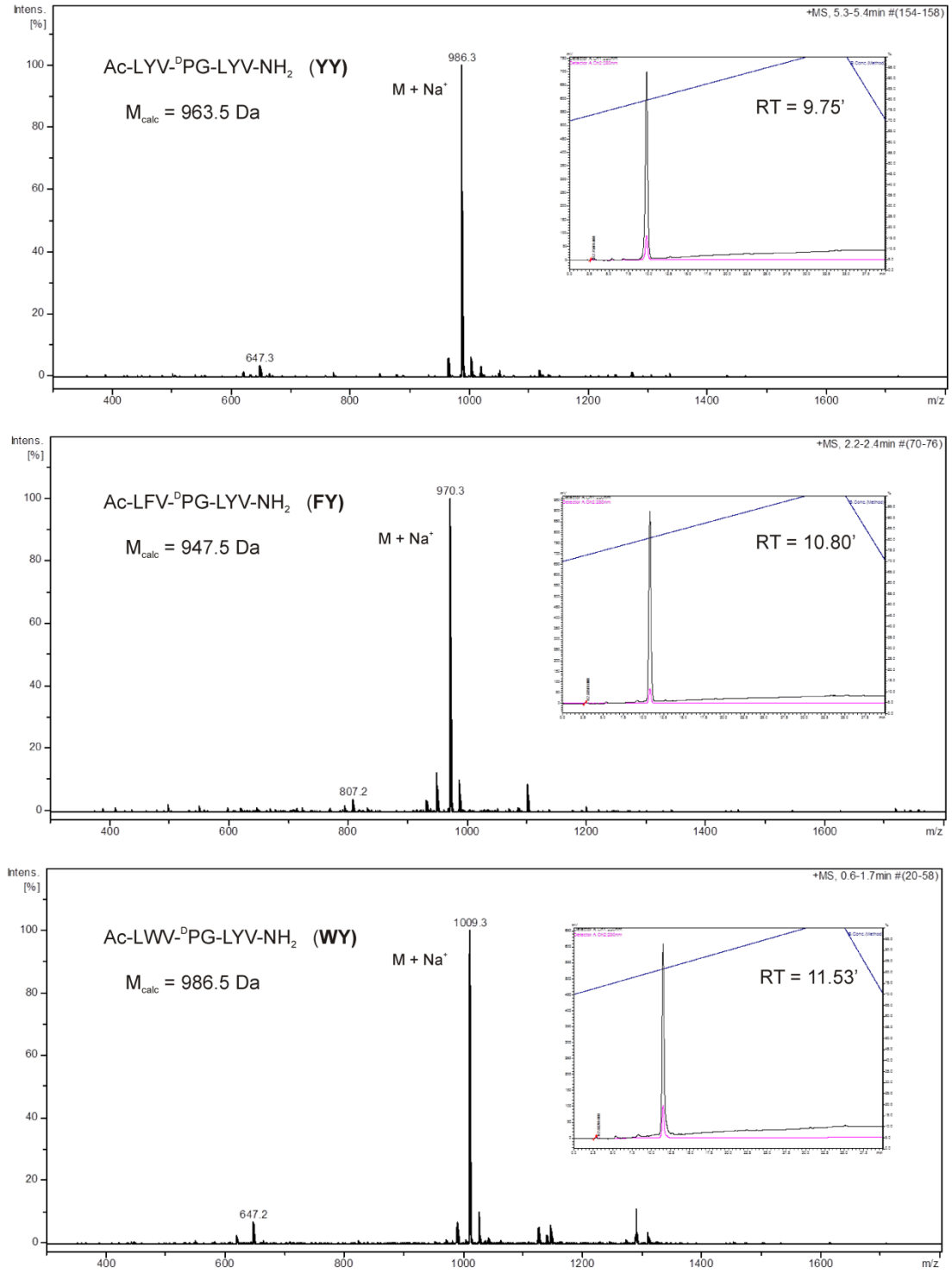

Fig. S1. Mass spectra and HPLC profiles. Mass spectra were recorded on Bruker Esquire 3000 Plus ion trap mass spectrometer. Calculated and observed masses of the peptides are highlighted. The sodiated species is the most prominent in all three peptides. The insets show analytical HPLC profiles of the respective peptides that were obtained on a Shimadzu UFLC system on a C_{18} reverse phase column (5 µm particle size) using a linear methanol-water gradient of 70-100% methanol over 30 min. Absorbance at 220 nm is in black and 280 nm profiles are in pink. The retention time (RT) of the peak of interest is indicated.

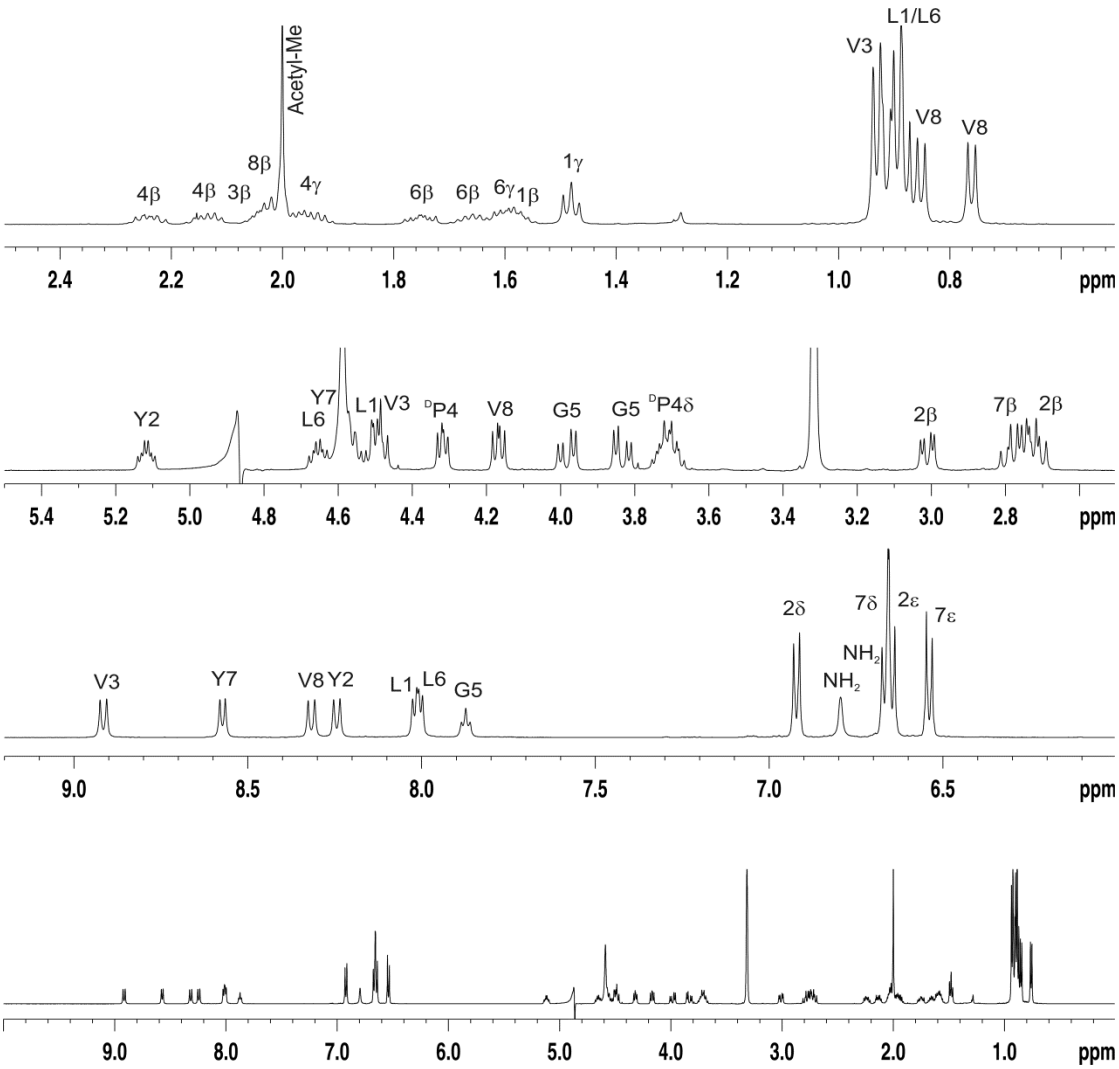

Residue	NH	$C^{\alpha}H$	$C^{\beta}H$	$C^{\gamma}H$	Others	$^{3}J_{NH\text{-}C^{\alpha}H}$	dδ/dT
	ppm	ppm	ppm	ppm	ppm	Hz	ppb/K
Leu1	8.02	4.51	1.59	1.48	$C^{\delta}H$: 0.92	8.69	-4.2
Tyr2	8.24	5.11	3.01 2.71	-	$C^{\delta}H$: 6.92 $C^{\varepsilon}H$: 6.64	9.12	-7.9
Val3	8.91	4.49	2.02	0.90	-	9.40	-4.2
^{D}Pro4	-	4.32	2.23 2.13	1.99	$C^{\delta}H$: 3.71	-	-
Gly5	7.87	3.98 3.83	-	-	-	-	-11.2
Leu6	8.00	4.65	1.75	1.59	$C^{\delta}H$: 0.90	8.69	-2.9
Try7	8.57	4.58	2.76	-	$C^{\delta}H$: 6.66 $C^{\varepsilon}H$: 6.53	8.00	-9.3
Val8	8.32	4.17	2.02	0.85 0.76	-	9.55	-1.9

Fig. S2. ^{1}H 1D spectrum (top) of peptide **YY** in CD_3OH at 303 K, showing complete resonance assignment and the corresponding NMR parameters (table, below) derived for this peptide.

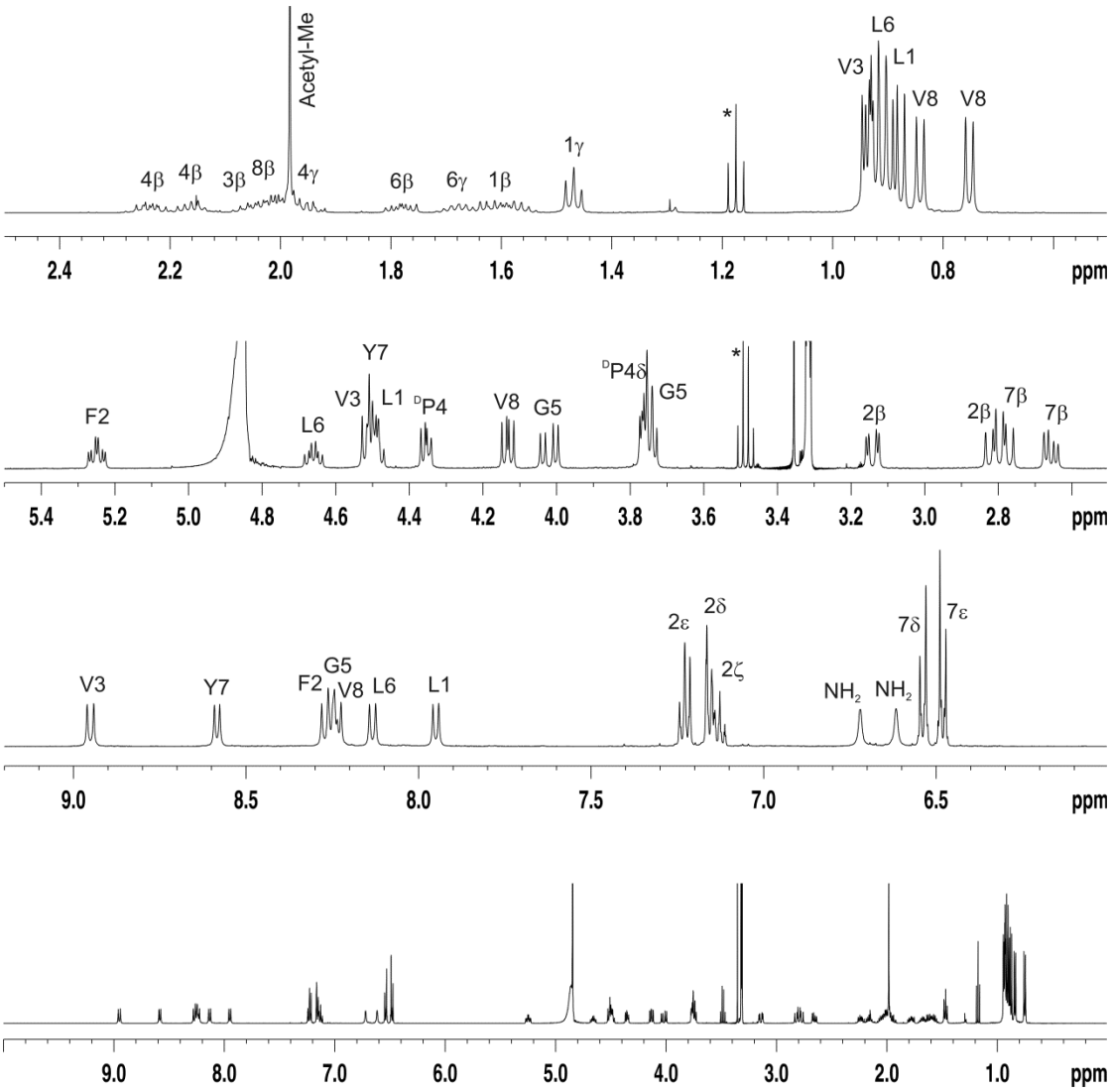

Residue	NH	$C^{\alpha}H$	$C^{\beta}H$	$C^{\gamma}H$	Others	$^{3}J_{NH\text{-}C^{\alpha}H}$	dδ/dT
	ppm	ppm	ppm	ppm	ppm	Hz	ppb/K
Leu1	7.95	4.49	1.56	1.47	$C^{\delta}H$: 0.89	8.35	-3.5
Phe2	8.27	5.25	3.14 2.81	-	$C^{\delta}H$: 7.16 $C^{\varepsilon}H$: 7.22 $C^{\zeta}H$: 7.12	9.31	-8.3
Val3	8.95	4.51	2.04	0.92	-	9.45	-4.6
^{D}Pro4	-	4.35	2.23	1.98	$C^{\delta}H$: 3.75	-	-
Gly5	8.24	4.02 3.75	-	-	-	-	-9.9
Leu6	8.13	4.66	1.78	1.63	$C^{\delta}H$: 0.92	8.98	-3.3
Try7	8.58	4.50	2.66 2.78	-	$C^{\delta}H$: 6.53 $C^{\varepsilon}H$: 6.48	7.70	-9.2
Val8	8.23	4.13	2.01	0.84 0.75	-	9.65	-2.5

Fig S3. ^{1}H 1D spectrum (top) of peptide **FY** in CD_3OH at 303 K, showing complete resonance assignment and the corresponding NMR parameters (table, below) derived for this peptide.

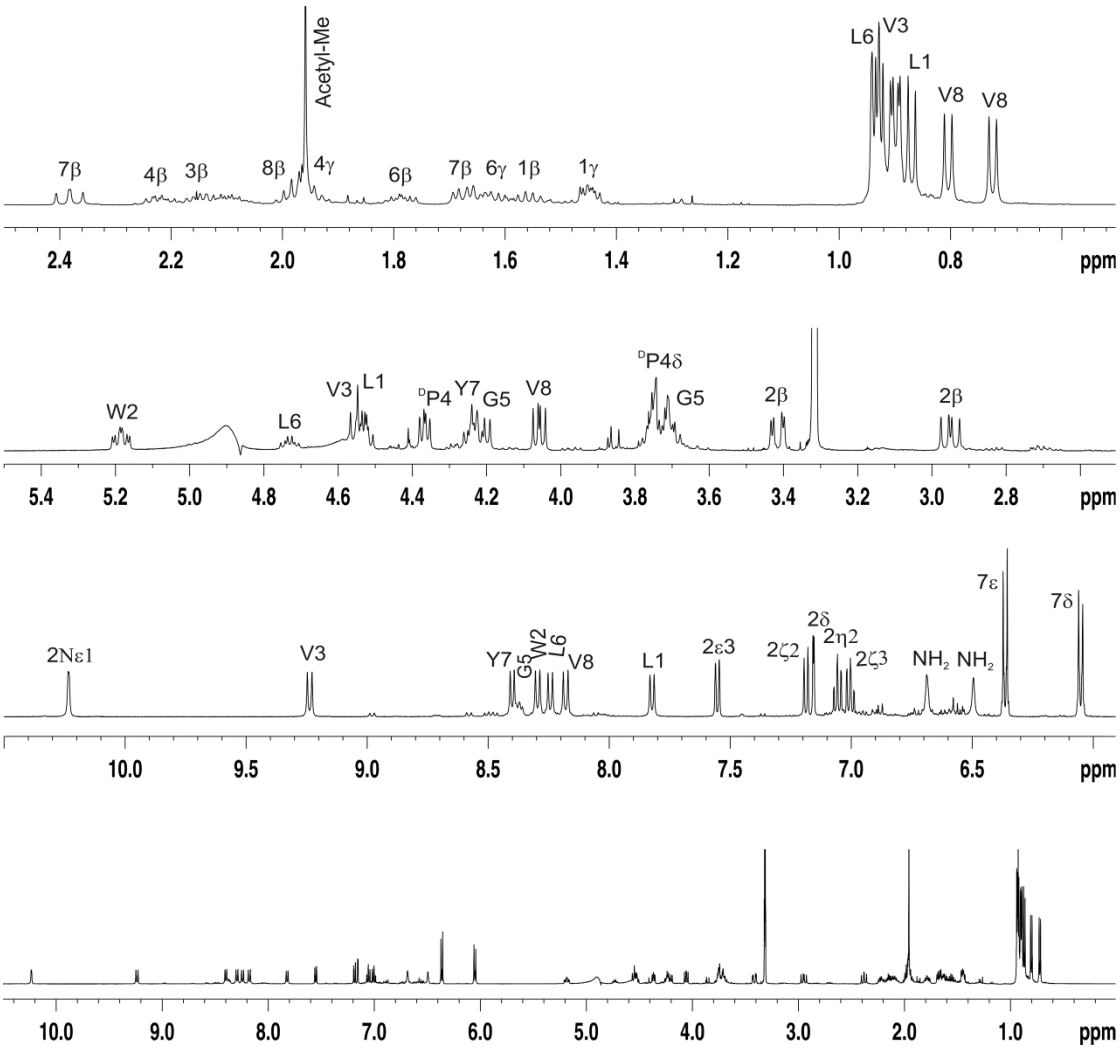

Residue	NH	$C^{\alpha}H$	$C^{\beta}H$	$C^{\gamma}H$	Others	$^{3}J_{NH\text{-}C^{\alpha}H}$	dδ/dT
	ppm	Ppm	ppm	ppm	ppm	Hz	ppb/K
Leu1	7.82	4.53	1.55	1.45	$C^{\delta}H$: 0.90	8.54	-3.5
Trp2	8.29	5.18	3.42 2.95	-	$C^{\delta 1}H$: 7.15 $N^{\varepsilon 1}H$: 10.23 $C^{\varepsilon 3}H$: $C^{\zeta 2}H$: 7.18 $C^{\zeta 3}H$: 7.00 $C^{\eta 2}H$: 7.05	9.05	-8.6
Val3	9.23	4.54	2.10	0.92	-	9.60	-6.3
DPro4	-	4.36	2.22	1.97	$C^{\delta}H$: 3.73	-	-
Gly5	8.36	4.21 3.73	-	-	-	-	-11.5
Leu6	8.24	4.73	1.78	1.63	$C^{\delta}H$: 0.91	9.26	-3.7
Try7	8.40	4.24	2.38 1.68	-	$C^{\delta}H$: 6.05 $C^{\varepsilon}H$: 6.36	8.16	-8.2
Val8	8.18	4.06	1.97	0.80 0.72	-	9.74	-1.8

Fig. S4. ^{1}H 1D spectrum (top) of peptide **WY** in CD_3OH at 303 K, showing complete resonance assignment and the corresponding NMR parameters (table, below) derived for this peptide.

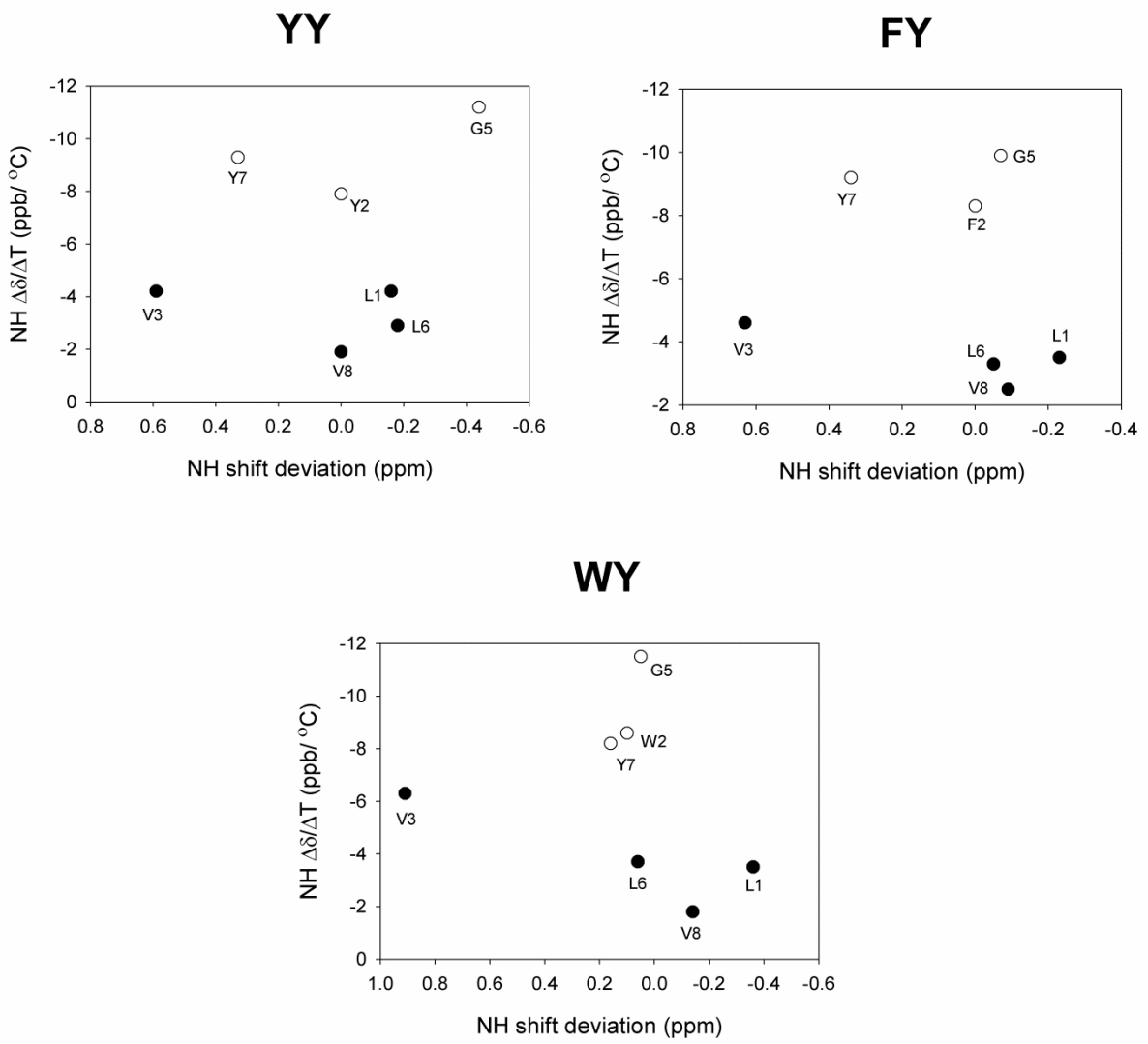

Fig. S5. Correlation plot of amide chemical shift deviation (CSD) against the temperature coefficient for all residues in the three peptides, except ^{D}Pro4. Residues that are expected to be hydrogen bonded in the β-hairpin scaffold are represented as filled circles and those involved in hydrogen bonding with the solvent (exposed amides), are indicated using open circles. Comparison with previous analyses from protein NMR data[1] provides us with an overall similarity in the expected dispersion of hydrogen bonded and non-hydrogen bonded amide resonances. However, detailed inference of the correlation coefficients in such systems is hampered by the highly dynamic nature of these molecules in solution.[1] Note that the Δδ/ΔT notation is used here for the *y*-axis, in accord with the original work.[1]

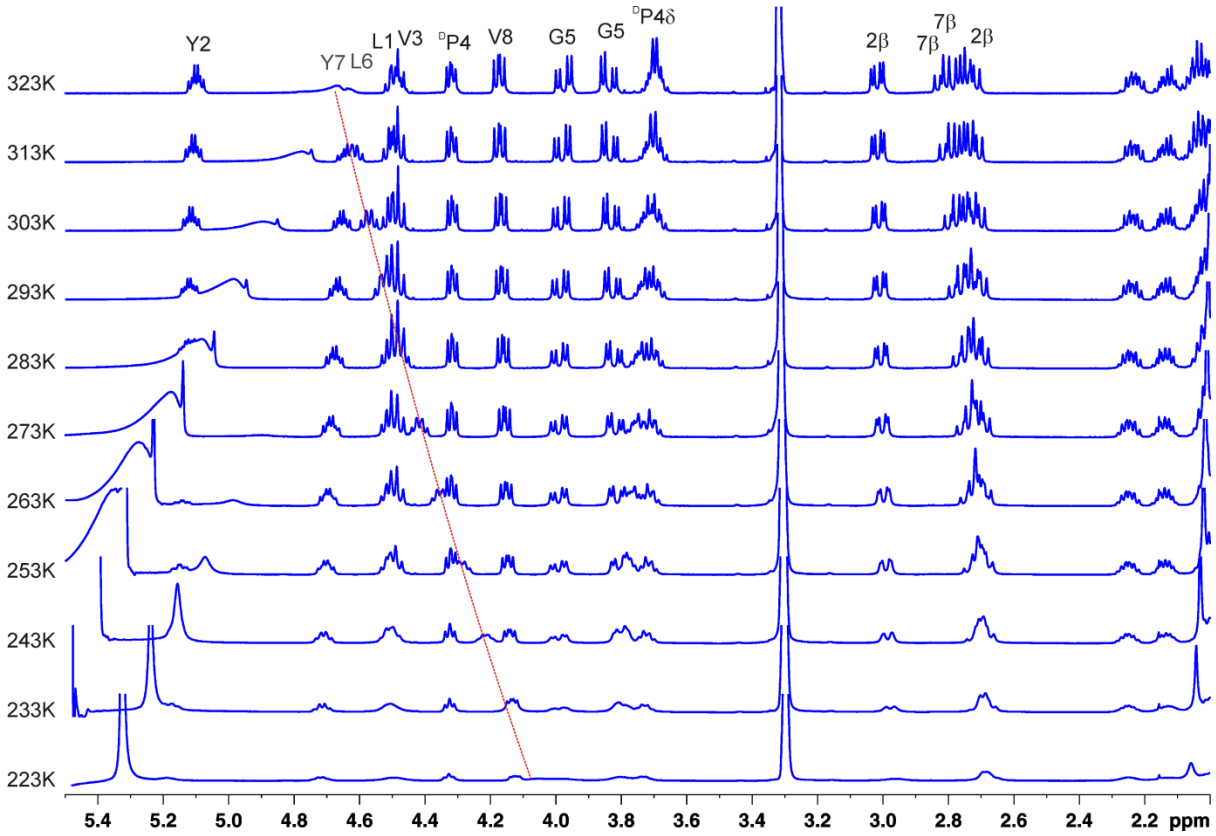

Fig. S6. ^{1}H 1D stack plot highlighting the resonances in the $C^{\alpha/\beta}H$ region in peptide **YY** in CD_3OH at various temperatures from 323 K to 223 K. Assignment of the various resonances is provided in the first spectrum. Notice that the Y7 $C^{\alpha}H$ displays a considerable temperature-dependence of its chemical shift, while the other $C^{\alpha}H$ resonances are largely invariant. Upfield shift of this resonance therefore arises from the shielding effect of the proximal aryl 2 ring; the extent of upfield shift can be considered as a qualitative indicator of the population of peptides bearing a spatially proximal aryl 2 – Tyr7 $C^{\alpha}H$ conformation. The pronounced upfield shift of this resonance upon lowering of temperature indicates greater ordering of the aryl side chains giving rise to increase in population of peptides bearing the T-shaped aromatic interactions, on the pre-formed β-hairpin scaffold.

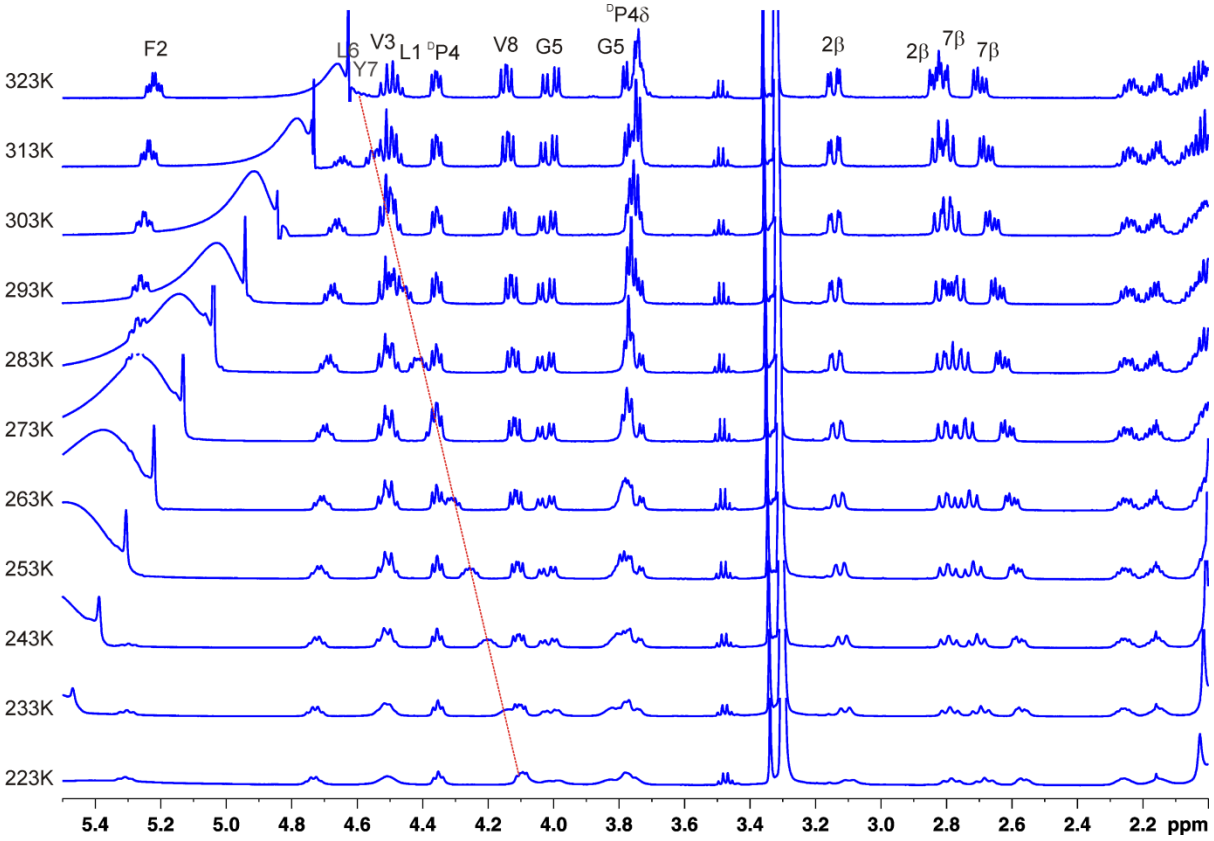

Fig. S7. ^{1}H 1D stack plot highlighting the resonances in the C$^{\alpha/\beta}$H region in peptide **FY** in CD_3OH at various temperatures from 323 K to 223 K. Assignment of the various resonances is provided in the first spectrum. As seen for **YY** in Fig. S6, the Y7 C$^{\alpha}$H displays a considerable temperature-dependence of its chemical shift, while the other C$^{\alpha}$H resonances are largely invariant. The upfield shift of this resonance upon lowering the temperature indicates an increase in the population of peptides bearing the T-shaped aromatic interactions, on the pre-formed β-hairpin scaffold.

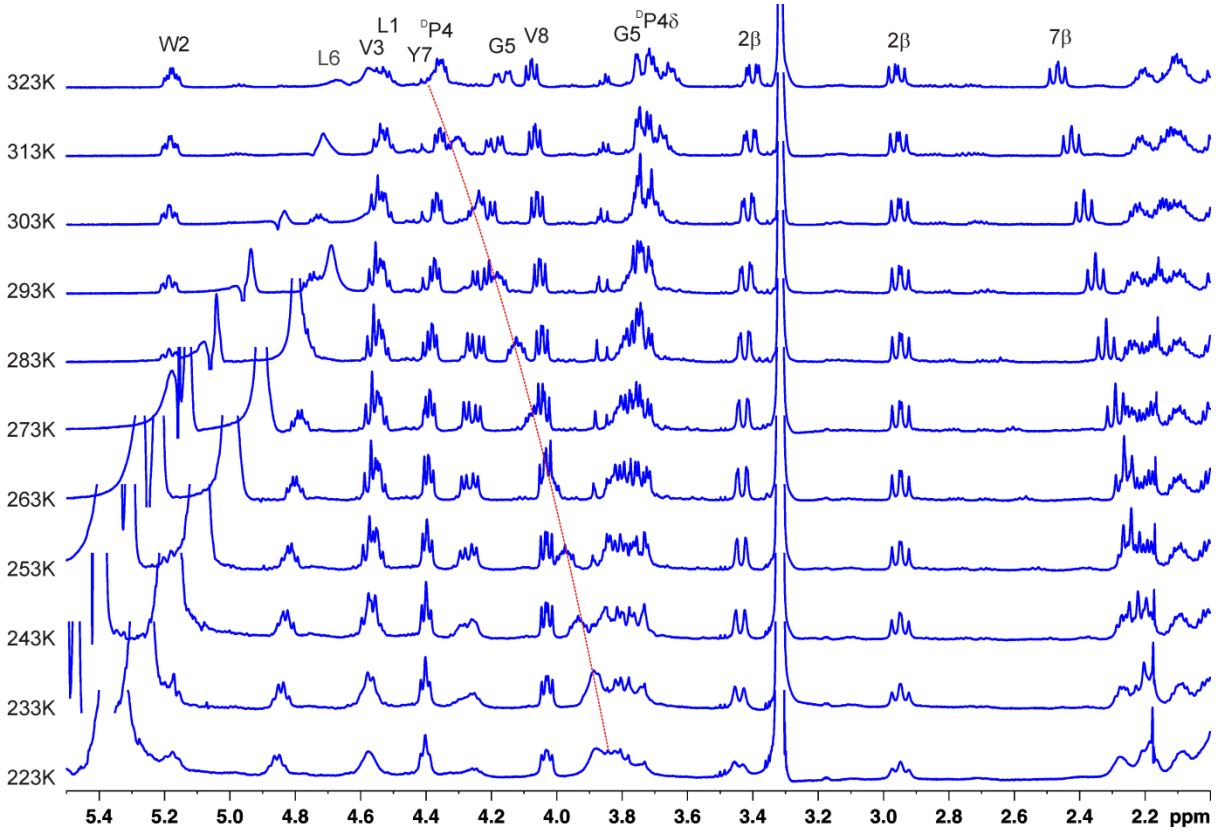

Fig. S8. ^{1}H 1D stack plot highlighting the resonances in the $C^{\alpha/\beta}H$ region in peptide **WY** in CD_3OH at various temperatures from 323 K to 223 K. Assignment of the various resonances is provided in the first spectrum. As seen for **YY** in Fig. S6 and **FY** in Fig. S7, the Y7 $C^{\alpha}H$ of this peptide also displays a considerable temperature-dependence of its chemical shift, while the other $C^{\alpha}H$ resonances are largely invariant. The upfield shift of this resonance upon lowering the temperature indicates an increase in the population of peptides bearing the T-shaped aromatic interactions, on the pre-formed β-hairpin scaffold.

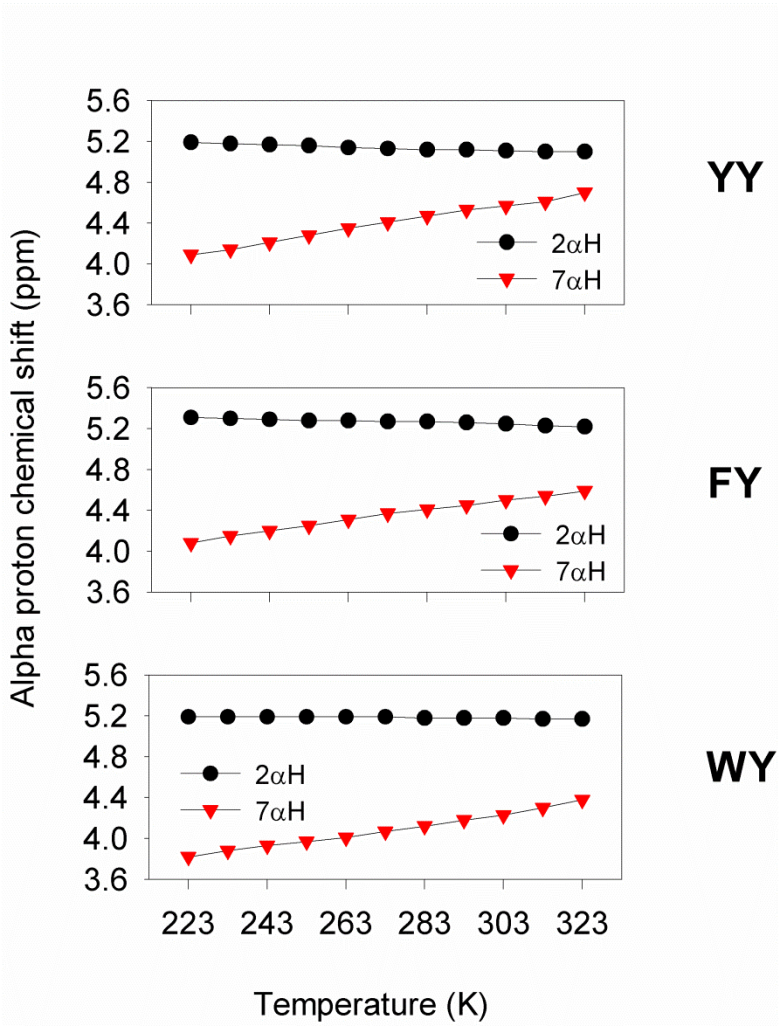

Fig. S9. Plot of the temperature dependence of the aryl 2 and Tyr7 CαH chemical shifts. Due to the T-shaped face-to-edge aromatic interaction geometry in all three peptides, the Tyr7 CαH falls under the shielding zone of the electron cloud of aryl 2 ring. Hence, it displays a temperature-dependent upfield shift from 323 K to 223 K, while the aryl 2 CαH is unaffected by temperature. The net chemical shift change over this temperature range ($\delta_{323} - \delta_{223}$) for the three peptides is as follows: Peptide **YY** :- Tyr2 CαH = -0.09 ppm, Tyr7 CαH = +0.61 ppm; Peptide **FY** :- Phe2 CαH = -0.09 ppm, Tyr7 CαH = +0.51 ppm; Peptide **WY** :- Trp2 CαH = -0.02 ppm, Tyr7 CαH = +0.56 ppm.

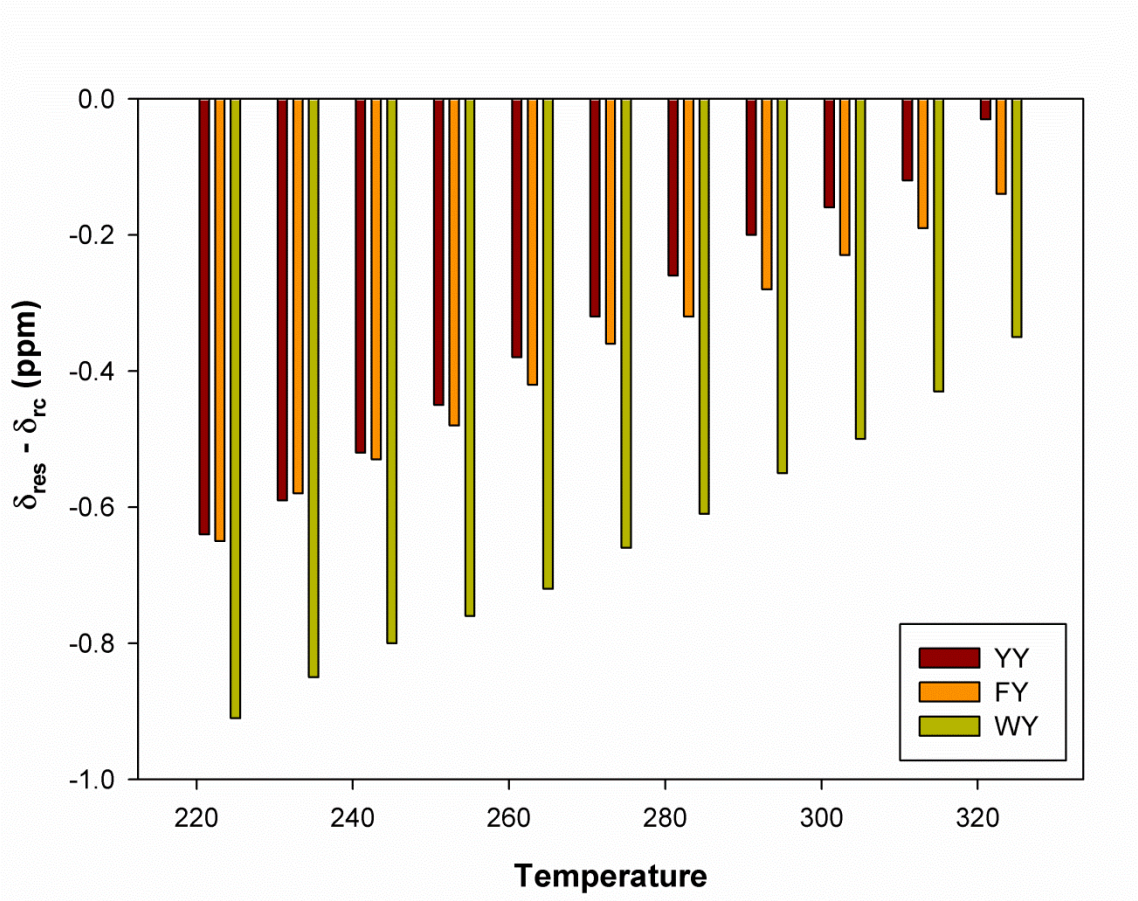

Fig. S10. Chemical shift indexing (CSI) of Tyr7 $C^{\alpha}H$ resonance with temperature, for the three peptides. The higher anomalous CSI values, which indicate strong influence of aromatic interactions, follow the order **WY**>**FY**≥**YY**. A similar trend was observed in our previous study using aryl 2 – Phe7 interactions in octapeptide β-hairpin scaffolds.[2]

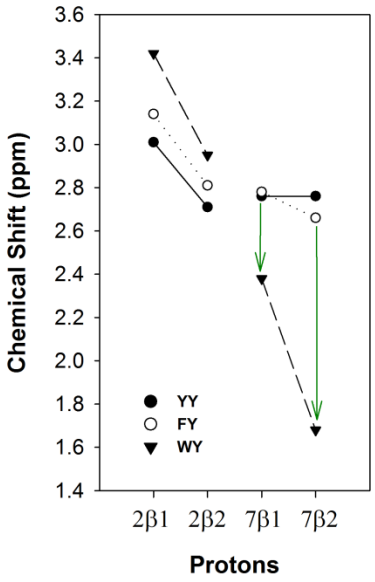

Fig. S11. Chemical shift comparison of the geminal $C^{\beta}H$ resonances of Tyr/Phe/Trp 2 and Tyr7 at 303 K. Notice the upfield shift of the one of the geminal Tyr7 $C^{\beta}H$ protons, when compared with the average chemical shift distribution of the corresponding aryl 2 protons. An additional anomalous upfield shift of ~0.4 ppm and ~1.0 ppm is seen in the case of the Tyr7 $C^{\beta}H$ resonances in **WY** (green drop arrows).

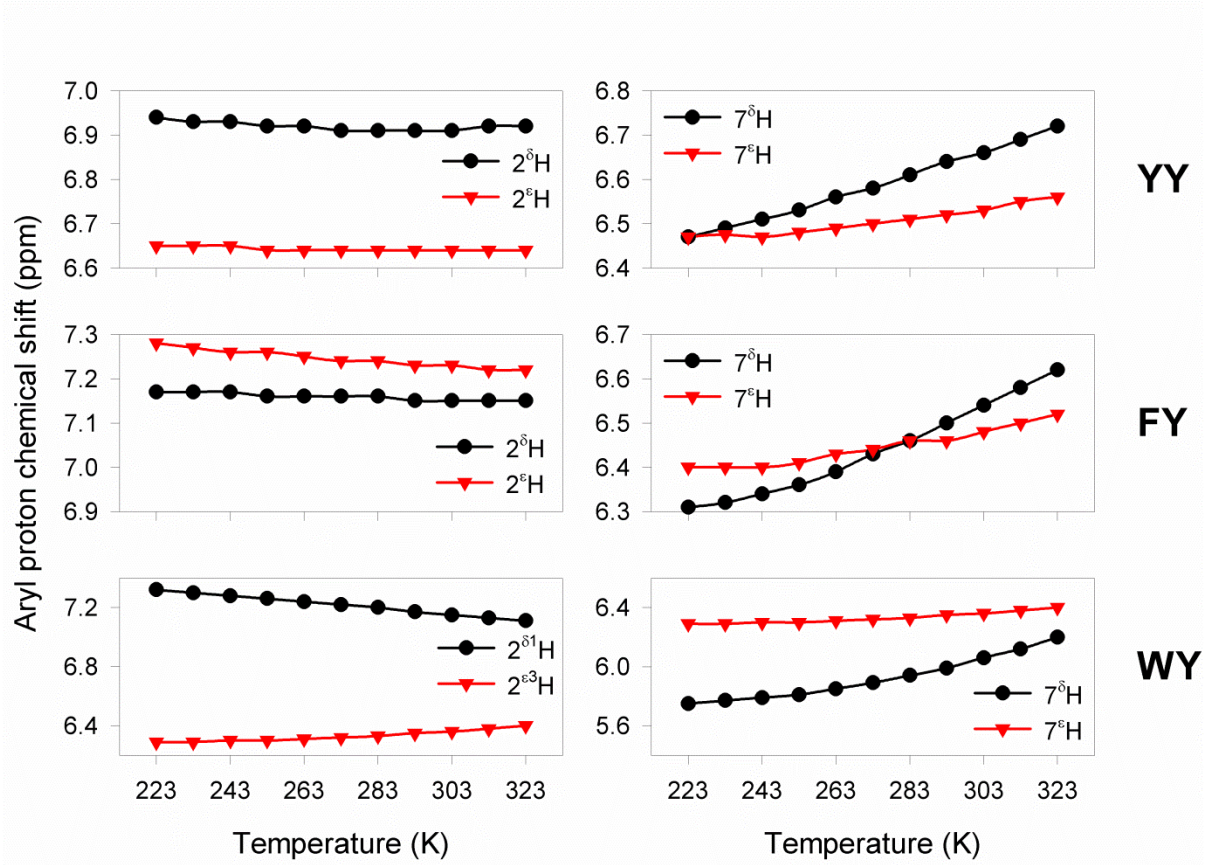

Fig. S12. Temperature-dependent aromatic ring proton chemical shifts. A prominent T-shape face-to-edge aromatic interaction results in shielding of characteristic edge ring proton, especially the Y7 $C^{\delta}H$ proton, and to lesser extent, the Y7 $C^{\varepsilon}H$ protons, in all three peptides studied herein. The corresponding $C^{\delta/\varepsilon}H$ resonances of residue 2 aryl ring (shown in the graphs on the left), are largely unaffected by temperature. Notice that the Y7 $C^{\delta}H$ resonance is upfield in the **WY** peptide, and indicates strong shielding effects from the spatially proximal indole ring.

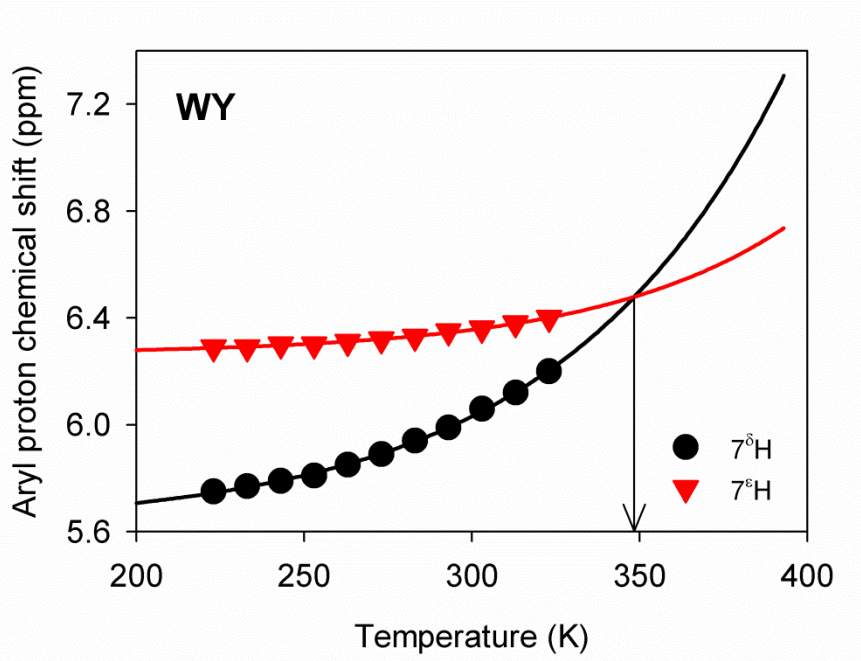

Fig. S13. Chemical shift values for Y7 $C^{\delta}H$ and Y7 $C^{\varepsilon}H$ protons in **WY,** obtained from the variable temperature proton 1D experiments, were extrapolated by fitting to an exponential function. The cross over point, which is highlighted by the drop-down arrow, is observed near 350 K. The expected random coil chemical shift of the Tyr $C^{\delta}H$ resonance is ~7.2 ppm. From the extrapolated values, this chemical shift is theoretically achieved at ~400 K (~125 °C). While random coil chemical shifts for this peptide may experimentally be obtainable at much lower temperatures, our data reflects the stability displayed by the Trp-Tyr interaction in the **WY** octapeptide.

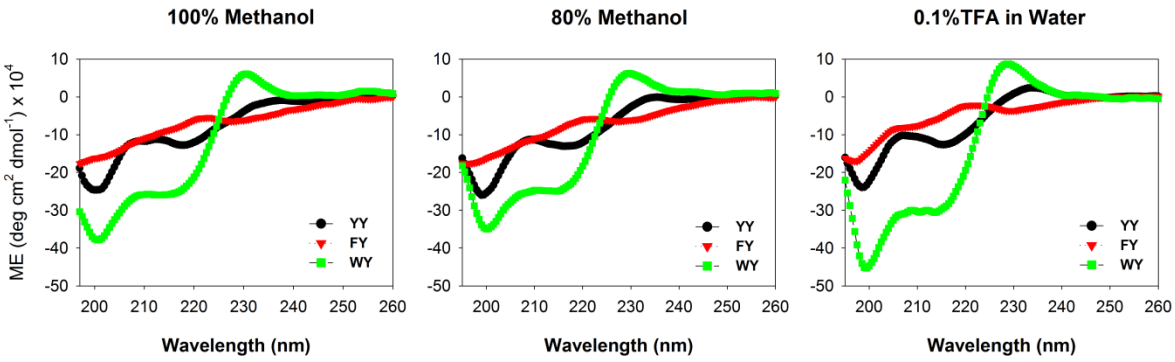

Fig. S14. Comparison of the far-UV CD spectra in solvent mixtures. Shown here are spectra acquired in methanol (left), methanol-water mixture (middle) and water (right) for **YY** (black), **FY** (red) and **WY** (green). All peptides posed difficulties while dissolving in water due to their largely apolar nature. Concentrations that were sufficient only for CD measurements were attained by extensive vortexing of the peptide powders in water containing 0.1% trifluoroacetic acid (TFA), followed by high speed centrifugation to remove particulate material. Quantification of the dissolved material in each solvent system was achieved using absorbance measurements. All CD spectra were acquired between 197-280 nm, on a J-815 CD spectropolarimeter (JASCO Inc.), using scan speeds of 100 nm/min, data pitch of 0.5nm, and averaged over three acquisitions. Blank subtracted smoothened data were converted to molar ellipticity values using reported methods. All spectra show substantial contributions from the aromatic residues; this masks the peptide backbone contributions to the CD spectrum, rendering meaningful deduction of peptide secondary structure from CD spectra, ineffective. Such substantial contributions of aromatic rings to the far-UV CD in such short sequences, is not uncommon, and has been observed earlier in both water-soluble peptides and hydrophobic sequences studied in organic solvents.[3] Shown here are the data acquired at 303K (30 °C). It is noteworthy that the CD profiles are largely unchanged across the three solvent conditions. Particularly, the retention of the exciton contributions of aryl rings in water could be considered as an indicator that a considerable population of these peptides molecules retain aromatic interactions, and could also be folded as β-hairpins.

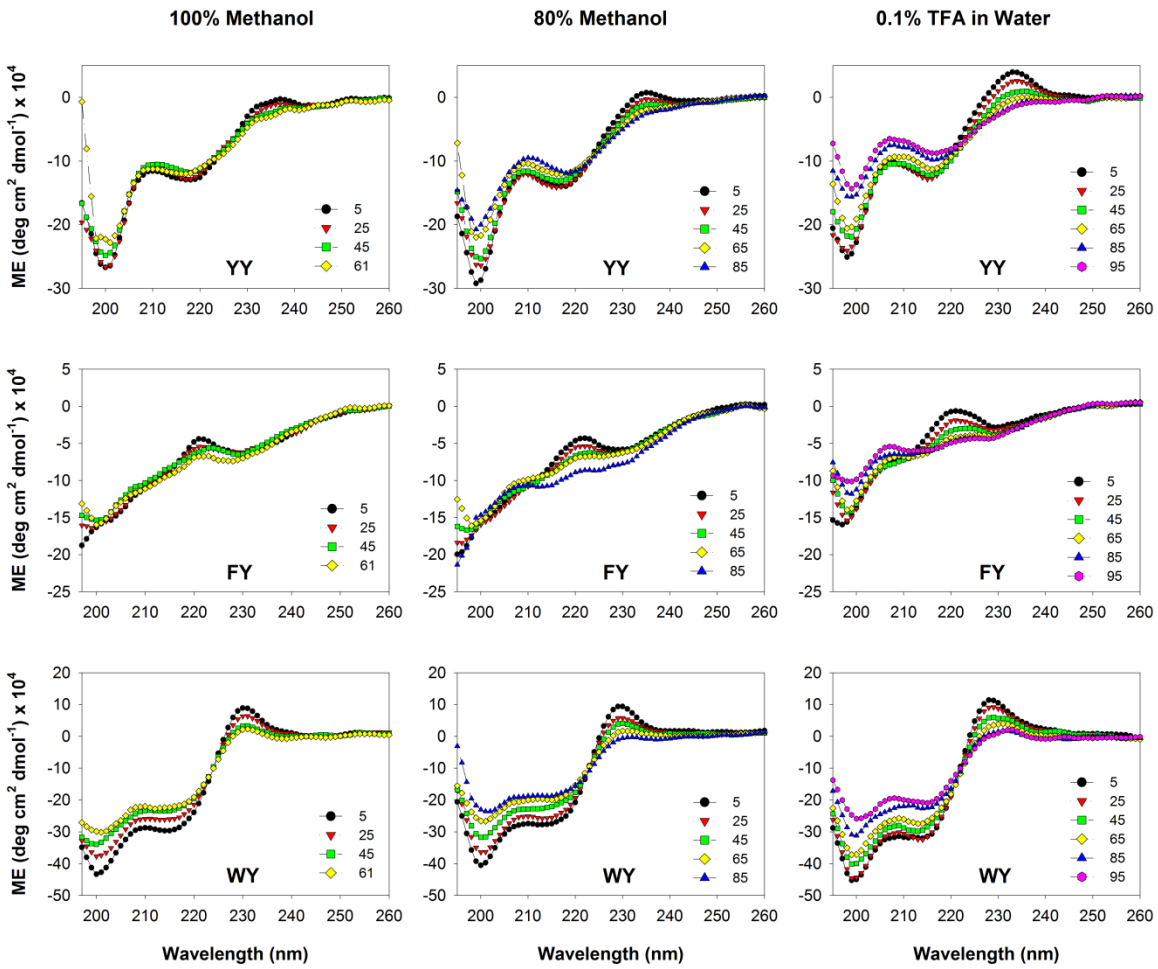

Fig. S15. Thermal denaturation measurements for peptides monitored with far-UV CD (continued from Fig. 7 of the main text). CD spectra were acquired as described in the legend to Fig. S14 at various temperatures from 5 °C to 71 °C in methanol (at 2 °C increments), 5 °C to 85 °C in 80% methanol (at 5 °C increments) and from 5 °C to 95 °C in water containing 0.1% TFA (at 5 °C increments). In the peptide **WY**, we observe a similar exciton coupling pattern and a temperature-dependent variation for this pattern, as has been observed previously for water-soluble peptide hairpins possessing Trp residues,[3b, 3c, 3e, 3f, 4] in all the three solvent conditions examined. **YY** and **FY** did not display significant changes in their CD profiles in methanol, upon changing the temperature. This could arise from the poorer contributions of tyrosine and phenylalanine to the far-UV CD, when compared with tryptophan or may also be due to the overall stability of these peptides under the conditions examined. In the absence of significant changes in the spectra, we could not derive meaningful conclusions from this experiment in methanol. Hence, we further assessed the aryl contributions to the far-UV CD in 80% methanol. Here, in the presence of water, we were able to achieve temperatures upto 85 °C. Again, **FY** displayed only marginal changes at ~221 nm. In water (containing 0.1% TFA), all three peptides displayed a temperature-dependent variation in the exciton coupling, which could be fitted to a sigmoidal function to derive the mid-point of this temperature-dependent transition (shown in Fig. S16).

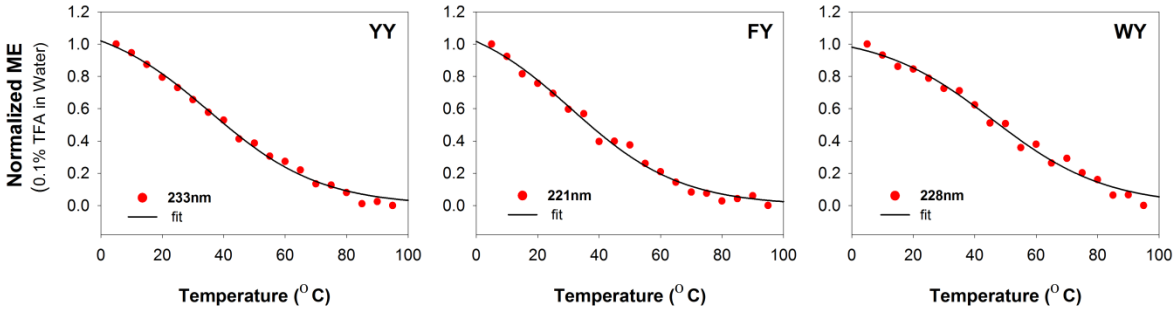

Fig. S16. Two-state unfolding of all peptides in water. Change in the CD spectra of the three peptides described in this study was plotted at 233 nm (for **YY**, left), 221 nm (for **FY**, middle) and 228 nm (for **WY**, right). These wavelengths were chosen based on the region at the red end of the observed CD profile, wherein we obtained a clean temperature-dependent change in the exciton coupling. The data were normalized and fitted to a sigmoidal function (fits shown as black solid lines in the figure) to obtain the mid-point of the thermal transition. We obtained values of ~41 °C for **YY**, ~37 °C for **FY** and ~49 °C for **WY** from the fits. This data provides us with a rank order of **WY>YY≈FY**, which is largely in agreement with our deductions from NMR experiments. However, as the magnitude of the exciton coupling heavily depends on whether one of the interacting pairs is a tryptophan, as well as the spatial positioning of the interacting aryl groups (for instance, see differences between **FY** and **YF** in Fig. S17), we strongly recommend caution while attempting to directly correlate the observed far-UV CD bands with folded β-hairpin populations and their associated stability.[5]

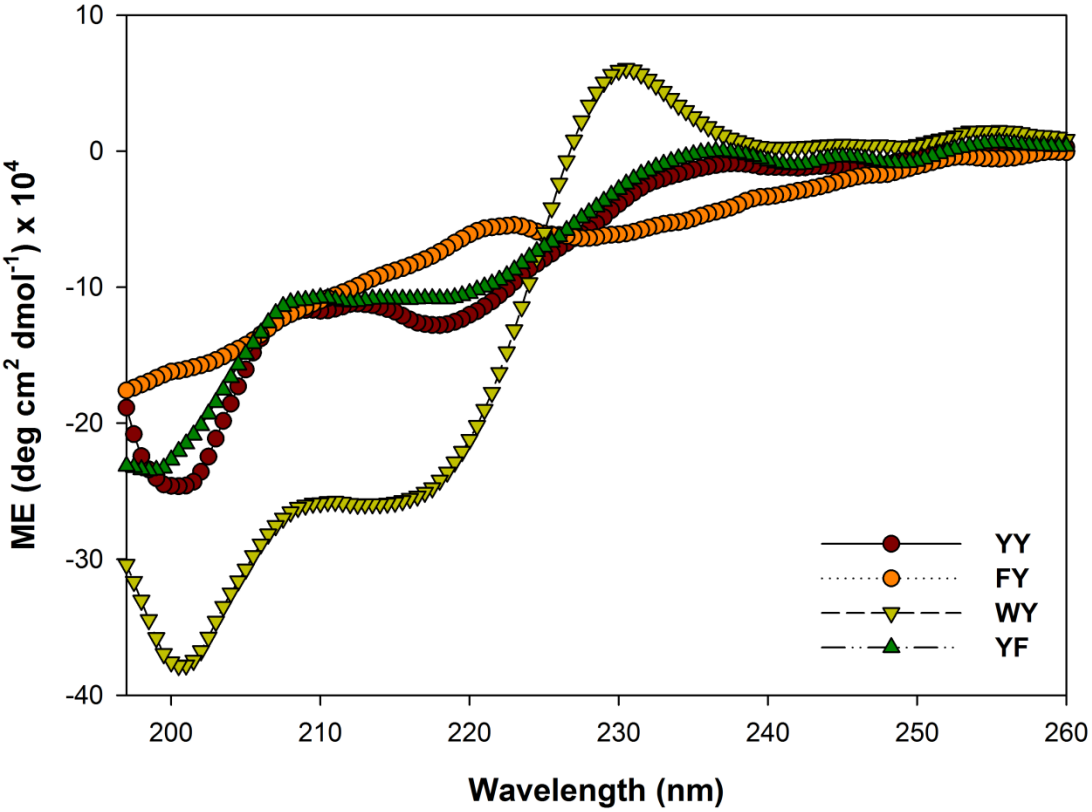

Fig. S17. Far-UV CD spectra in methanol at 300 K (27 °C). Spectra were acquired as described in the legend to Fig. S14. All spectra show substantial contributions from the aromatic residues, rendering meaningful deduction of peptide secondary structure from CD spectra, ineffective.[3] However, in our data, it is interesting to note that the variation in aryl conformational geometry can contribute significantly and differently to the CD spectrum. This is best illustrated by the comparison of the observed spectra of **FY** (this study) and **YF** peptides.[2, 3h]

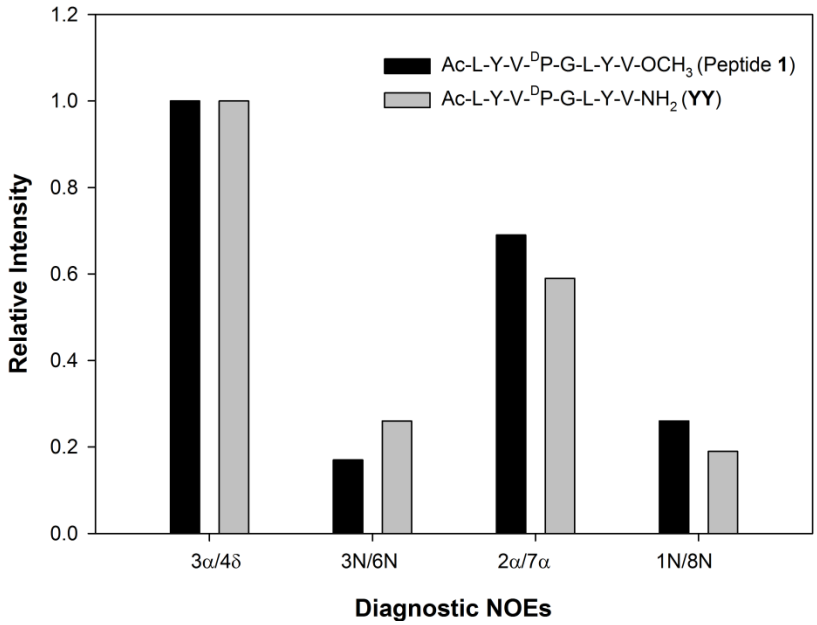

Fig. S18. Comparison of diagnostic β-hairpin NOE intensities across octapeptide hairpins containing Tyr-Tyr interactions. NOE intensities from homonuclear ^{1}H-^{1}H 2D-ROESY spectra for peptide **1** (Ac-LYV-^{D}PG-LYV-OCH_3)[3d] were calculated from Fig. 4 of ref. 3d by densitometry analysis using MultiGauge v2.3, as reported earlier.[3g] A similar calculation was carried out for the peptide **YY** (Ac-LYV-^{D}PG-LYV-NH_2, this study). All values were normalized against the intensity of $3^{\alpha}\leftrightarrow4^{\delta}$ NOE. Lowering of the cross-strand $2^{\alpha}\leftrightarrow7^{\alpha}$ and 1N↔8N NOEs indicate greater strand fraying in **YY**, despite better turn stabilization (3N↔6N NOE).

Supporting Tables

Table S1: Summary of the experimental constraints used to calculate the NMR structures.

Experimental constraints	**No. of constraints**		
	YY	**FY**	**WY**
Intraresidue NOEs	38	38	40
Sequential NOEs	16	15	15
Long range NOEs	22	25	23
Hydrogen bonds	4	4	4
Angle constraints	12	12	12
Results			
Violations observed in the calculated 100 structures.	0	0	0

Table S2: Average backbone torsional angles calculated for the first 35 structures.

Ac-L-Y-V-^{D}P-G-L-Y-V-$CONH_2$, **YY**		
Residue	Phi[a]	Psi[a]
Leu 1	-	78.9 +/- 4.2
Tyr 2	-122.6 +/- 1.7	143.8 +/- 1.6
Val 3	-139.5 +/- 0.8	71.5 +/- 1.6
^{D}Pro 4	69.8 +/- 0.03	-114.1 +/- 0.8
Gly 5	-90.2 +/- 0.1	15.9 +/- 0.3
Leu 6	-139.4 +/- 2.9	162.3 +/- 1.5
Tyr 7	-124.6 +/- 5.0	157.2 +/- 0.2
Val 8	-120.0 +/- 0.0	-

[a]Values are provided in degrees.

Ac-L-F-V-^{D}P-G-L-Y-V-$CONH_2$, **FY**		
Residue	Phi[a]	Psi[a]
Leu 1	-	74.6 +/- 9.0
Phe 2	-126.5 +/- 6.3	135.6 +/- 8.0
Val 3	-133.3 +/- 5.6	74.7 +/- 1.5
^{D}Pro 4	69.8 +/- 0.03	-114.0 +/- 2.3
Gly 5	-90.4 +/- 0.1	16.6 +/- 0.6
Leu 6	-136.1 +/- 3.5	164.5 +/- 1.8
Tyr 7	-129.9 +/- 7.4	147.1 +/- 2.7
Val 8	-125.2 +/- 7.7	-

[a]Values are provided in degrees.

Ac-L-W-V-^{D}P-G-L-Y-V-$CONH_2$, **WY**		
Residue	Phi[a]	Psi[a]
Leu 1	-	84.7 +/- 0.3
Trp 2	-99.1 +/- 0.2	125.4 +/- 1.9
Val 3	-125.9 +/- 1.3	75.7 +/- 1.7
^{D}Pro 4	69.8 +/- 0.03	-112.1 +/- 1.6
Gly 5	-91.5 +/- 0.2	16.2 +/- 3.5
Leu 6	-128.4 +/- 3.6	142.2 +/- 1.8
Tyr 7	-119.0 +/- 0.3	144.2 +/- 0.6
Val 8	-140.2 +/- 0.3	-

[a]Values are provided in degrees.

Table S3: List of experimental distance constraints used to derive the structure of **YY** shown in Fig. 5A.

1	LEU				
	H	1	LEU	HA	5.0
	H	1	LEU	QB	3.5
	H	1	LEU	HG	3.5
	H	1	LEU	QQD	5.0
	HA	1	LEU	QB	3.5
	H	2	TYR	H	3.5
	HA	2	TYR	H	2.5
	H	8	VAL	H	5.0
	H	7	TYR	QD	5.0
2	TYR				
	H	2	TYR	HA	5.0
	H	2	TYR	QB	3.5
	H	2	TYR	QD	5.0
	HA	2	TYR	QB	3.5
	HA	2	TYR	QD	3.5
	HA	2	TYR	QE	5.0
	QB	2	TYR	QD	3.5
	QB	2	TYR	QE	5.0
	QB	3	VAL	H	3.5
	QD	2	TYR	QE	2.5
	HA	3	VAL	H	2.5
	QD	3	VAL	H	5.0
	HA	7	TYR	HA	3.0
	HA	7	TYR	QD	5.0
	HA	7	TYR	QE	5.0
	HA	8	VAL	H	5.0
#	QD	5	GLY	QA	5.0
	QD	7	TYR	HA	5.0
	QE	7	TYR	HA	5.0
	QD	7	TYR	QD	5.0
	QD	7	TYR	QE	5.0
	QD	7	TYR	H	5.0
	QD	6	LEU	HA	5.0
	QD	6	LEU	H	5.0
#	QD	4	DPRO	QD	5.0
#	QB	4	DPRO	QD	5.0
	QD	7	TYR	QB	5.0
	QE	7	TYR	QB	3.5
3	VAL				
	H	3	VAL	HA	5.0
	H	3	VAL	HB	3.5
	H	3	VAL	QQG	3.5
	HA	3	VAL	HB	3.5
	H	6	LEU	H	3.5
	H	6	LEU	QB	5.0
	HA	4	DPRO	QD	2.5
	H	7	TYR	HA	5.0
	H	4	DPRO	QD	5.0
4	DPRO				
	HA	4	DPRO	QB	2.5
	QB	4	DPRO	QD	5.0
	QG	4	DPRO	QD	2.5
	HA	5	GLY	H	2.5
	HA	6	LEU	H	5.0
	QB	5	GLY	H	5.0
5	GLY				
	H	5	GLY	QA	5.0
	H	6	LEU	H	3.5
	QA	6	LEU	H	3.5
6	LEU				
	H	6	LEU	HA	5.0
	H	6	LEU	QB	3.5
	H	6	LEU	HG	3.5
	H	6	LEU	QQD	5.0
	HA	6	LEU	QB	3.5
	HA	7	TYR	H	2.5
	HG	7	TYR	H	5.0
7	TYR				
	H	7	TYR	HA	5.0
	H	7	TYR	QB	3.5
	H	7	TYR	QD	5.0
	HA	7	TYR	QB	3.5
	HA	7	TYR	QD	3.5
	QB	7	TYR	QD	3.5
	HA	8	VAL	H	2.5
	QD	8	VAL	H	5.0
	QE	8	VAL	HB	5.0
8	VAL				
	H	8	VAL	HA	5.0
	H	8	VAL	HB	3.5
	H	8	VAL	QQG	3.5
	HA	8	VAL	HB	3.5
	HA	8	VAL	QQG	3.5

NOEs unsuited for this particular conformation (corresponding to Tyr2 χ_1 = *-gauche*) were deleted (highlighted in red) and a separate structure calculation (100 structures) was carried out.

Table S4: List of experimental distance constraints used to derive the structure of **YY** shown in Fig. 5B.

1	LEU				
	H	1	LEU	HA	5.0
	H	1	LEU	QB	3.5
	H	1	LEU	HG	3.5
	H	1	LEU	QQD	5.0
	HA	1	LEU	QB	3.5
	H	2	TYR	H	3.5
	HA	2	TYR	H	2.5
	H	8	VAL	H	5.0
	H	7	TYR	QD	5.0
2	TYR				
	H	2	TYR	HA	5.0
	H	2	TYR	QB	3.5
	H	2	TYR	QD	5.0
	HA	2	TYR	QB	3.5
	HA	2	TYR	QD	3.5
	HA	2	TYR	QE	5.0
	QB	2	TYR	QD	3.5
	QB	2	TYR	QE	5.0
	QB	3	VAL	H	3.5
	QD	2	TYR	QE	2.5
	HA	3	VAL	H	2.5
	QD	3	VAL	H	5.0
	HA	7	TYR	HA	2.5
	HA	7	TYR	QD	5.0
	HA	7	TYR	QE	5.0
	HA	8	VAL	H	5.0
	QD	5	GLY	QA	5.0
	QD	7	TYR	HA	5.0
	QE	7	TYR	HA	5.0
	QD	7	TYR	QD	5.0
	QD	7	TYR	QE	5.0
	QD	7	TYR	H	5.0
	QD	6	LEU	HA	5.0
	QD	6	LEU	H	5.0
	QD	4	DPRO	QD	5.0
	QB	4	DPRO	QD	5.0
	QD	7	TYR	QB	5.0
	QE	7	TYR	QB	3.5
3	VAL				
	H	3	VAL	HA	5.0
	H	3	VAL	HB	3.5
	H	3	VAL	QQG	3.5
	HA	3	VAL	HB	3.5
	H	6	LEU	H	3.5
	H	6	LEU	QB	5.0
	HA	4	DPRO	QD	2.5
	H	7	TYR	HA	5.0
	H	4	DPRO	QD	5.0
4	DPRO				
	HA	4	DPRO	QB	2.5
	QB	4	DPRO	QD	5.0
	QG	4	DPRO	QD	2.5
	HA	5	GLY	H	2.5
	HA	6	LEU	H	5.0
	QB	5	GLY	H	5.0
5	GLY				
	H	5	GLY	QA	5.0
	H	6	LEU	H	3.5
	QA	6	LEU	H	3.5
6	LEU				
	H	6	LEU	HA	5.0
	H	6	LEU	QB	3.5
	H	6	LEU	HG	3.5
	H	6	LEU	QQD	5.0
	HA	6	LEU	QB	3.5
	HA	7	TYR	H	2.5
	HG	7	TYR	H	5.0
7	TYR				
	H	7	TYR	HA	5.0
	H	7	TYR	QB	3.5
	H	7	TYR	QD	5.0
	HA	7	TYR	QB	3.5
	HA	7	TYR	QD	3.5
	QB	7	TYR	QD	3.5
	HA	8	VAL	H	2.5
	QD	8	VAL	H	5.0
	QE	8	VAL	HB	5.0
8	VAL				
	H	8	VAL	HA	5.0
	H	8	VAL	HB	3.5
	H	8	VAL	QQG	3.5
	HA	8	VAL	HB	3.5
	HA	8	VAL	QQG	3.5

Table S5: List of experimental distance constraints used to derive the structure of **YY** shown in Fig. 5C.

1	LEU				
	H	1	LEU	HA	5.0
	H	1	LEU	QB	3.5
	H	1	LEU	HG	3.5
	H	1	LEU	QQD	5.0
	HA	1	LEU	QB	3.5
	H	2	TYR	H	3.5
	HA	2	TYR	H	2.5
	H	8	VAL	H	5.0
	H	7	TYR	QD	5.0
2	TYR				
	H	2	TYR	HA	5.0
	H	2	TYR	QB	3.5
	H	2	TYR	QD	5.0
	HA	2	TYR	QB	3.5
	HA	2	TYR	QD	3.5
	HA	2	TYR	QE	5.0
	QB	2	TYR	QD	3.5
	QB	2	TYR	QE	5.0
	QD	2	TYR	QE	2.5
	HA	3	VAL	H	2.5
	QD	3	VAL	H	5.0
	HA	7	TYR	HA	2.5
	HA	7	TYR	QD	5.0
	HA	7	TYR	QE	5.0
	HA	8	VAL	H	5.0
	QE	5	GLY	QA	5.0
	QD	7	TYR	HA	5.0
	QE	7	TYR	HA	5.0
#	QD	7	TYR	QD	5.0
#	QD	7	TYR	QE	5.0
#	QE	7	TYR	QD	5.0
	QD	7	TYR	H	5.0
	QD	6	LEU	HA	5.0
	QD	6	LEU	H	5.0
	QD	4	DPRO	QD	3.5
	QB	4	DPRO	QD	5.0
	QD	7	TYR	QB	5.0
	QE	7	TYR	QB	3.5
3	VAL				
	H	3	VAL	HA	5.0
	H	3	VAL	HB	3.5
	H	3	VAL	QQG	3.5
	HA	3	VAL	HB	3.5
	H	6	LEU	H	3.5
	H	6	LEU	QB	5.0
	HA	4	DPRO	QD	2.5
	H	7	TYR	HA	5.0
	H	4	DPRO	QD	5.0
4	DPRO				
	HA	4	DPRO	QB	2.5
	QB	4	DPRO	QD	5.0
	QG	4	DPRO	QD	2.5
	HA	5	GLY	H	2.5
	HA	6	LEU	H	5.0
	QB	5	GLY	H	5.0
5	GLY				
	H	5	GLY	QA	5.0
	H	6	LEU	H	3.5
	QA	6	LEU	H	3.5
6	LEU				
	H	6	LEU	HA	5.0
	H	6	LEU	QB	3.5
	H	6	LEU	HG	3.5
	H	6	LEU	QQD	5.0
	HA	6	LEU	QB	3.5
	HA	7	TYR	H	2.5
	HG	7	TYR	H	5.0
7	TYR				
	H	7	TYR	HA	5.0
	H	7	TYR	QB	3.5
	H	7	TYR	QD	5.0
	HA	7	TYR	QB	3.5
	HA	7	TYR	QD	3.5
	QB	7	TYR	QD	3.5
	HA	8	VAL	H	2.5
	QD	8	VAL	H	5.0
	QE	8	VAL	HB	5.0
8	VAL				
	H	8	VAL	HA	5.0
	H	8	VAL	HB	3.5
	H	8	VAL	QQG	3.5
	HA	8	VAL	HB	3.5
	HA	8	VAL	QQG	3.5

NOEs unsuited for this particular conformation (corresponding to Tyr2 χ_1 = *trans*) were deleted (highlighted in red) and a separate structure calculation (100 structures) was carried out.

References

1. N. H. Andersen, J. W. Neidigh, S. M. Harris, G. M. Lee, Z. H. Liu and H. Tong, *J. Am. Chem. Soc.*, 1997, **119**, 8547-8561.
2. K. M. Makwana and R. Mahalakshmi, *Org. Biomol. Chem.*, 2014, **12**, 2053-2061.
3. (a) C. X. Zhao, P. L. Polavarapu, C. Das and P. Balaram, *J. Am. Chem. Soc.*, 2000, **122**, 8228-8231; (b) A. G. Cochran, N. J. Skelton and M. A. Starovasnik, *Proc. Natl. Acad. Sci. U. S. A.*, 2001, **98**, 5578-5583; (c) C. D. Tatko and M. L. Waters, *J. Am. Chem. Soc.*, 2002, **124**, 9372-9373; (d) R. Mahalakshmi, S. Raghothama and P. Balaram, *J. Am. Chem. Soc.*, 2006, **128**, 1125-1138; (e) L. Wu, D. McElheny, R. Huang and T. A. Keiderling, *Biochemistry*, 2009, **48**, 10362-10371; (f) L. Wu, D. McElheny, T. Takekiyo and T. A. Keiderling, *Biochemistry*, 2010, **49**, 4705-4714; (g) K. M. Makwana, S. Raghothama and R. Mahalakshmi, *Phys. Chem. Chem. Phys.*, 2013, **15**, 15321-15324; (h) K. M. Makwana and R. Mahalakshmi, *ChemBioChem*, 2014, **15**, 2357-2360.
4. (a) S. Russell and A. G. Cochran, *J. Am. Chem. Soc.*, 2000, **122**, 12600-12601; (b) M. L. Waters, *Curr. Opin. Chem. Biol.*, 2002, **6**, 736-741; (c) R. M. Hughes and M. L. Waters, *Curr. Opin. Struct. Biol.*, 2006, **16**, 514-524; (d) L. Wu, D. McElheny, V. Setnicka, J. Hilario and T. A. Keiderling, *Proteins*, 2012, **80**, 44-60.
5. R. Mahalakshmi, G. Shanmugam, P. L. Polavarapu and P. Balaram, *ChemBioChem*, 2005, **6**, 2152-2158.